Electric Power Systems Research 81 (2011) 1805–1814

Contents lists available at ScienceDirect

Electric Power Systems Research

journal homepage: www.elsevier.com/locate/epsr

Voltage imbalance analysis in residential low voltage distribution networks with rooftop PVs

Farhad Shahnia[a,*], Ritwik Majumder[b], Arindam Ghosh[a], Gerard Ledwich[a], Firuz Zare[a]

[a] Engineering Systems School, Faculty of Built Environment and Engineering, Queensland University of Technology, Brisbane, Australia
[b] Power Technology Group of ABB Corporate Research, Sweden

ARTICLE INFO

Article history:
Received 23 August 2010
Received in revised form 15 April 2011
Accepted 1 May 2011
Available online 28 May 2011

Keywords:
Distribution network
Sensitivity analysis
Single-phase rooftop PV
Stochastic evaluation
Voltage imbalance

ABSTRACT

The installation of domestic rooftop photovoltaic cells (PVs) are on the rise due to feed-in tariff and changes driven by environmental concerns. Even though the increase in the PV installation is gradual, their locations and ratings are often random. Therefore, such single-phase bi-directional power flow can have adverse effect on the voltage imbalance of a three-phase distribution network. In this paper, a voltage imbalance sensitivity analysis and stochastic evaluation based on the ratings and locations of single-phase grid-connected rooftop PVs in a residential low voltage distribution network are presented. The stochastic evaluation, based on Monte Carlo method, predicts a failure index of non-standard voltage imbalance in the network in presence of PVs. Some improvement methods are discussed and a new improvement method based on PV converter control is proposed.

1. Introduction

Current and voltage imbalance is one of the power quality problems in low voltage (LV) distribution networks [1]. Voltage imbalance is more common in individual customer loads due to phase load imbalances, especially where large single-phase power loads are used [2]. Although voltages are well balanced at the supply side, the voltages at the customer level can become unbalanced due to the unequal system impedances, unequal distribution of single-phase loads or large number of single-phase transformers [2]. Usually, the electric utilities aim to distribute the residential loads equally among the three phases of distribution feeders [3].

An increase in the voltage imbalance can result in overheating and de-rating of all induction motor types of loads [4]. Voltage imbalance can also cause network problems such as mal-operation of protection relays and voltage regulation equipment, and generation of non-characteristic harmonics from power electronic loads [3].

In recent years, there is a growing interest by the residential customers in the installation of single-phase grid-connected rooftop Photovoltaic cells (PVs) due to new energy and incentive polices in several countries [5]. The most important characteristic of these PVs is that their output power being fed to the grid is not controlled and is dependent on the instantaneous power from the sun. Several technical problems of these systems such as harmonics, voltage profile and power loss are already studied and investigated in [6–8].

The residential rooftop PVs are currently installed randomly across distribution systems. This may lead to an increase in the imbalance index of the network. This will increasingly cause problems for three-phase loads (e.g. motors for pumps and elevators). Refs. [9,10] have investigated some technical problems of European and UK distribution networks for maximum allowable number of grid-connected PVs. However there is a need to investigate the sensitivity analysis of voltage imbalance in these networks.

A deterministic analysis may not be suitable given the randomness of PV installations and their intermittent nature of power generation. Monte Carlo method is already applied for analysis of uncertainties in the network in order to study load flow, voltage sag, fault and reliability [11]. Therefore, a stochastic evaluation based on Monte Carlo method is carried out in this paper to investigate and predict the network voltage imbalance for the uncertainties arising due to rooftop PV power ratings and locations. Later, some voltage imbalance mitigation methods are discussed and a new method is proposed.

2. Voltage imbalance

Voltage imbalance in the three-phase electric system is a condition in which the three phase voltages differ in amplitude and/or does not have its normal 120° phase difference. There have been several methods for definition, calculation and interpretation of Voltage Unbalance Factor (VUF) as proposed in [12–14]. IEEE

* Corresponding author. Tel.: +61 432020732.
E-mail addresses: f.shahnia@qut.edu.au, shahniafarhad@yahoo.com (F. Shahnia).

0378-7796/$ – see front matter © 2011 Elsevier B.V. All rights reserved.
doi:10.1016/j.epsr.2011.05.001

Recommended Practice for Monitoring Electric Power Quality defines this as [15]

$$\text{VUF\%} = \left|\frac{V_-}{V_+}\right| \times 100 \quad (1)$$

where V_- and V_+ are the negative and positive sequence of the voltage, respectively. This will be referred to as percentage voltage imbalance in the paper.

According to [15], the allowable limit for voltage imbalance is limited to 2% in low voltage and medium voltage networks. Engineering Recommendation P29 in UK not only limits the whole voltage imbalance of the network to 2%, but also limits the voltage imbalance to 1.3% at the load point [16]. ANSI standard for "Electric Power Systems and Equipment Voltage Ratings (60 Hz)" recommends that electrical supply systems should be designed and operated to limit the maximum voltage imbalance to 3% when measured at the electric utility end points under no-load conditions [17].

IEEE Recommended Practice for Electric Power Systems in Commercial Buildings (Gray Book) indicates that the single-phase power electronics based devices like the computers, entertainment equipment, etc. may experience problems if the voltage imbalance is more than 2–2.5% where the voltage amplitudes exceed the limits [18].

The voltage imbalance has adverse effect on the three-phase power electronic based equipment in the network [19,20] (e.g. central speed variable air conditioners). It will also have adverse effect on the operating characteristics of three-phase induction motors used in water pumps, elevators, etc. in residential apartment complex [5].

3. Voltage imbalance in LV distribution networks with PVs

The utilities try to minimize the imbalance index in their network by distributing single-phase loads equally across all three phases. Probabilistic studies have shown that it is very rare that the residential and small business loads can result in higher values of the voltage imbalance in the network. The measurements done in a LV distribution network in US [19], Brazil [20] and Iran [21] conclude that the probability of the voltage imbalance to be more than 3% in the network is about 2–5%. However, this can only be achieved if the engineering judgements have been applied for selecting the appropriate size of the conductors and cables, transformer ratings and also if the load dispatch among the three phases are recorrected by later observations and measurements. If the appropriate designs have not been done or there is a non-standard voltage drop in the network, it is highly probable that the network also suffers from higher voltage imbalance.

As mentioned before, rooftop PVs that are currently being installed depend on outlook and financial condition of householders. Therefore, it is not unexpected that these installations are randomly placed along distribution feeders. For example, it is possible that 80% of customers on a phase have installed PVs, while the other two phases have only 50% and 10% installed. In such a condition, even if the voltage imbalance of the network was within the standard limits without any PVs, it is not guaranteed to remain so. Therefore, the possible PV installation number or rating on such systems must be investigated in a way that the voltage imbalance is still kept within the standard limit.

3.1. Network structure

A sample radial LV residential urban distribution network is considered for voltage imbalance investigations. The simplified equivalent single line diagram of one feeder of the network is illustrated in Fig. 1. In this model, the PVs are all grid-connected such that the surplus of the electricity generated will flow to the grid. It has been assumed that all the PVs work at unity power factor based on IEEE Recommended Practice for Utility Interface of Photovoltaic Systems [22]. It is also assumed that the neutral conductor is making the pass for unbalance current circulation and the analysis is based on the mutual effect of three phases.

3.2. Power flow analysis

For calculating the voltage imbalance, it is necessary that the network to be analysed and the voltages at the desired nodes to be calculated. Based on the KCL on each node of phase *A*, we have for

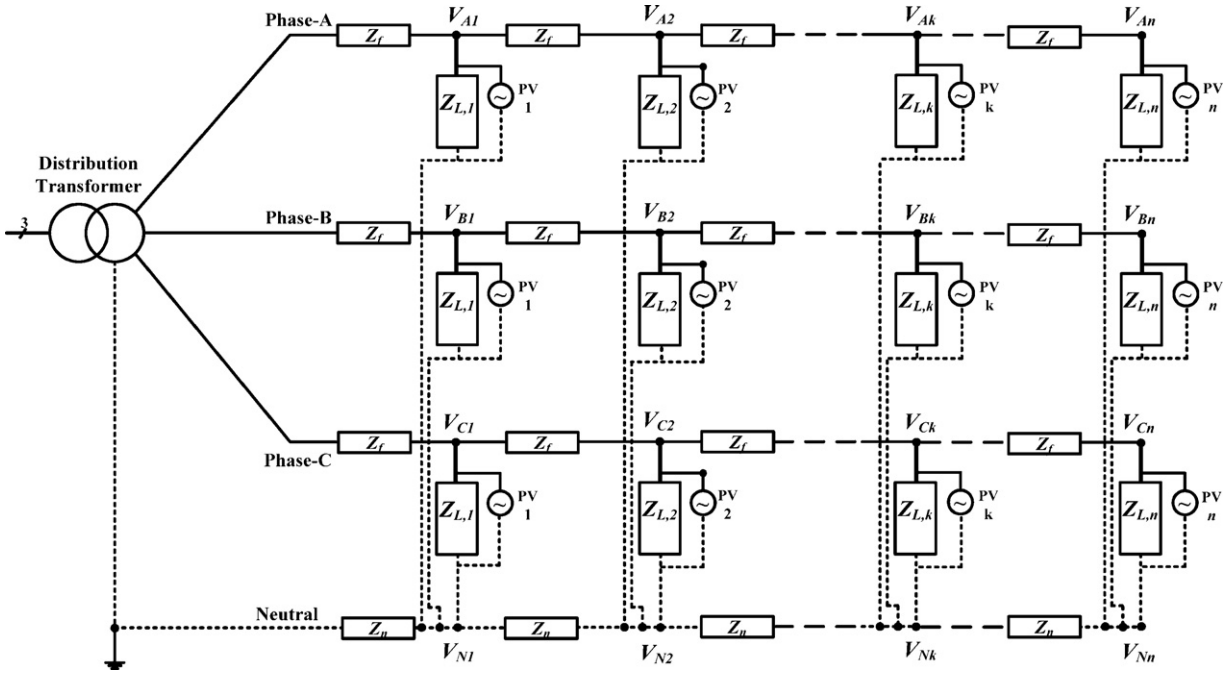

Fig. 1. Schematic single line diagram of one feeder of the studied LV distribution network.

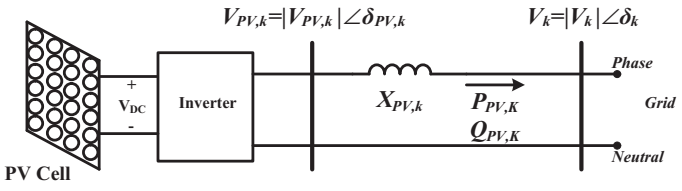

Fig. 2. Schematic diagram of a PV connection to grid.

the kth node

$$\frac{\beta(V_{A,PV,k}-V_{A,k})}{X_{A,PV,k}}+\frac{V_{A,k-1}-V_{A,k}}{Z_f}+\frac{V_{A,k+1}-V_{A,k}}{Z_f}+\frac{V_{N,k}-V_{A,k}}{Z_{A,L,k}}=0 \tag{2}$$

where Z_f is the feeder impedance between two adjacent nodes in phase lines, $V_{A,i}$, $i=1,\ldots,n$ is the single-phase voltage of the ith node of phase A, $Z_{A,L,k}$ is the load impedance connected to kth node of phase A and and $V_{N,k}$ is the voltage of the neutral wire connected to kth node. $V_{A,PV,k}$ and $X_{A,PV,k}$ are the PV voltage and impedance connected to kth node of phase A. Similar equations are valid for phases B and C. In (2), the controlling constant β is equal to 1 when there is a PV connected to kth node, otherwise, it is zero.

KCL for each node on the neutral line is

$$\frac{V_{N,k-1}-V_{N,k}}{Z_n}+\frac{V_{N,k+1}-V_{N,k}}{Z_n}+\frac{V_{N,k}-V_{A,k}}{Z_{A,L,k}}+\frac{V_{N,k}-V_{B,k}}{Z_{B,L,k}}+\frac{V_{N,k}-V_{C,k}}{Z_{C,L,k}}=0 \tag{3}$$

where Z_n is the feeder impedance between two adjacent nodes in neutral line.

The simplified diagram of the PV connection to the grid is shown in Fig. 2. Based on this figure, we have

$$P_{PV,k}=\frac{|V_{PV,k}||V_k|}{|X_{PV,k}|}\sin(\delta_{PV,k}-\delta_k) \tag{4}$$

$$Q_{PV,k}=\frac{|V_k|}{|X_{PV,k}|}(|V_{PV,k}|\cos(\delta_{PV,k}-\delta_k)-|V_k|) \tag{5}$$

where $P_{PV,k}$ and $Q_{PV,k}$ are respectively the active and reactive power output of the PV connected to kth node. Assuming $P_{PV,k}$ and $Q_{PV,k}$ to be constant and $|V_k|$ and δ_k are known, $|V_{PV,k}|$ and $\delta_{PV,k}$ can be calculated. Please note that $Q_{PV,k}$ will be zero if the PV operates in Unity Power Factor (UPF).

To calculate V_k from (2) to (5), an iterative method is required. Starting with a set of initial values, the entire network is solved to determine V_k. Once the solution converges, the sequence components are calculated. These sequence components are later used to voltage imbalance calculation given in (1).

3.3. Sensitivity analysis

The voltage at any node can be considered as a function of the location and rating of PV. Therefore the sensitivity of network voltage imbalance to a PV location and rating is expressed as

$$S_k=\frac{\partial \mathrm{VUF}}{\partial P_{PV,k}}\frac{P_{PV,k}}{\mathrm{VUF}} \tag{6}$$

Since voltages at each node are calculated iteratively, the sensitivity is calculated numerically once the iterations converge as

$$S_k=\frac{\mathrm{VUF}(\gamma+1)-\mathrm{VUF}(\gamma)}{P_{PV,k}(\gamma+1)-P_{PV,k}(\gamma)} \tag{7}$$

where $0\le\gamma\le4$ defines the rating of the PV (i.e. 0, 1, 2, 3, 4, 5 kW).

3.4. Stochastic evaluation

Monte Carlo simulation is a powerful numerical method of stochastic evaluation based on random input variables [11].

The inherent characteristic of LV distribution networks includes random variation of residential load demand and PV power generation at different time periods. This variation is based on load demand in about 12 h sunshine daily pattern and summer–winter periods. In addition to this, the random location and nominal power of PVs increase the randomness of the network.

For investigating the voltage imbalance in the network when there is a random combination of rooftop PVs with different ratings and at different location on all phases and feeders on the network, a stochastic evaluation based on Monte Carlo method has been carried out. Three random inputs of the stochastic evaluation are the number of householders with installed rooftop PVs, the ratings of the PVs and their location in the different phases and feeders. The flowchart of Monte Carlo method is shown in Fig. 3. In this figure, the inputs are network (load, feeder and transformer) data. The random number generation and selection of the other parameters for the Monte Carlo method is explained in Section 4.3. For each set of data, the load flow is carried out and voltage imbalance is calculated.

The expected VUF at the calculation node $\overline{\mathrm{VUF}}_j$ from each trial $1\le k\le N$, is calculated by

$$\overline{\mathrm{VUF}}_j=\frac{1}{N}\sum_{k=1}^{N}\mathrm{VUF}_k \tag{8}$$

The unbiased sample variance for VUF at the calculated nodes (beginning or end of feeder) is as follows:

$$\mathrm{Var}(\mathrm{VUF}_j)=\frac{1}{N-1}\sum_{k=1}^{N}(\mathrm{VUF}_k-\overline{\mathrm{VUF}}_j)^2 \tag{9}$$

The stopping rule of the Monte Carlo method is chosen based on achieving an acceptable convergence for $\overline{\mathrm{VUF}}$ and Var(VUF). In this study, the number of Monte Carlo trials is chosen as $N=10{,}000$ to achieve an acceptable convergence. This is more explained in Appendix A.

The voltage imbalance results as the output of the Monte Carlo simulations are used to calculate the Probability Density Function (PDF) and the average (mean value) of all VUFs which is shown as λ in the paper.

4. Numerical results

A sample radial LV (415 V) residential urban distribution network is considered for voltage imbalance investigations. This network is supposed to supply electricity to a combination of residential and small business customers. It has three feeders, each three-phase and 4-wire system with equal length (400 m) and equal number of customers on each phase and feeder. The poles are located at a distance of almost 40 m from each other. At each pole, 2 houses are supplied from each phase. The feeders and their cross-section are also designed appropriately based on the amount of power and the voltage drop. The technical data of the network is given in Appendix A.

It is assumed that the total electric demand of the network is almost 1 MVA including the LV network under consideration that is supplying a total demand of 360 kW. It is also assumed that during the period of study the loads of phases A, B and C are 60, 120 and 180 kW, respectively. The rest of the network load (the portion not included in this study) is considered as a lumped load. The rooftop PVs installed by the householders have an output power in

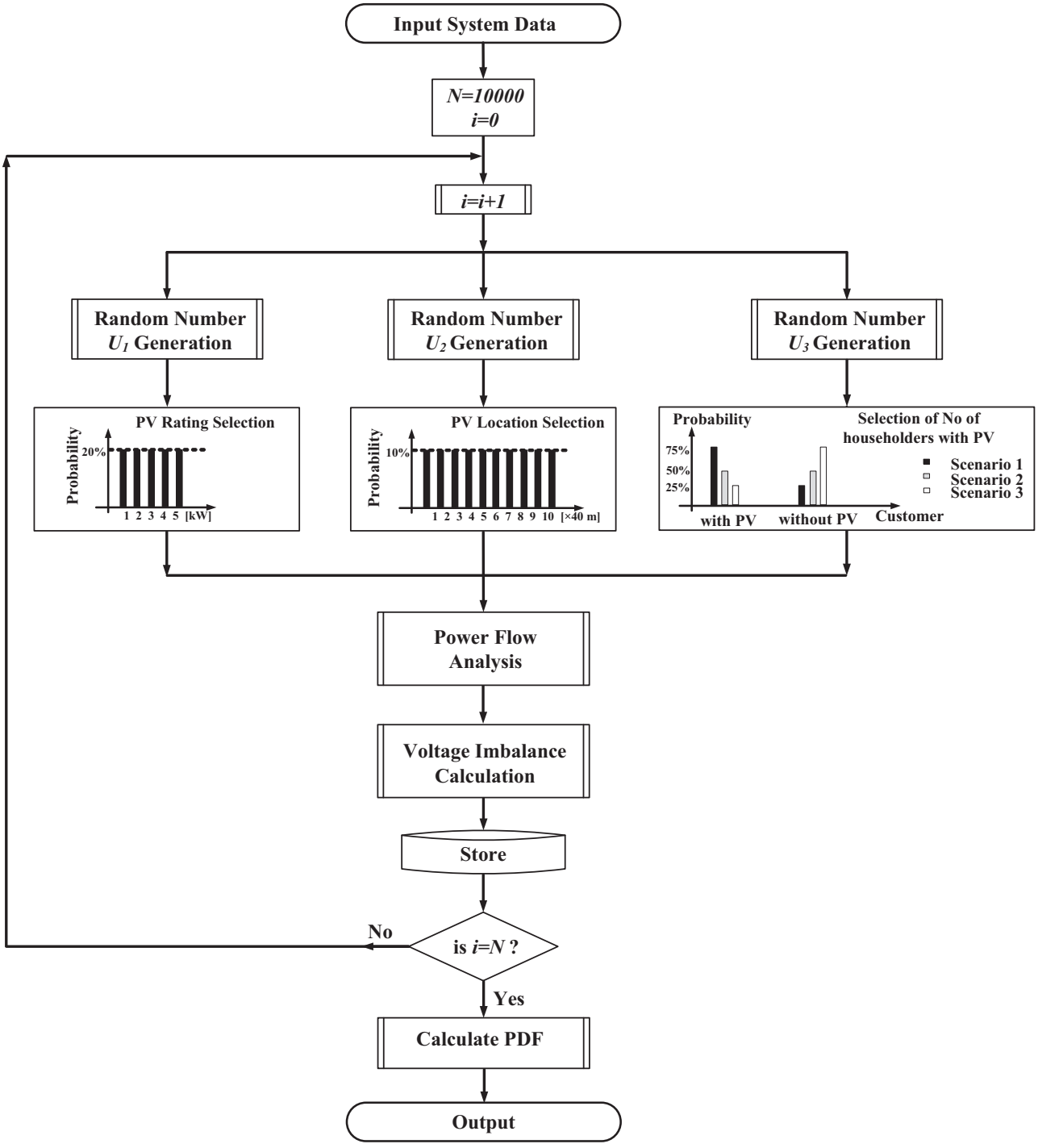

Fig. 3. Monte Carlo flowchart for stochastic evaluation.

the range of 1–5 kW working in unity power factor. Several studies are performed, which are discussed below.

The utilities usually measure and monitor the voltage imbalance at the beginning of the feeder (i.e. secondary side of the distribution transformer). As described previously, the probabilistic studies of the measurement results show that there is low chance of having a voltage imbalance beyond 2% at this location. Let us assume that the length of the three phases and number of customers per phase are the same. Even then, since the power consumption of the loads is different, there will be different voltage drops along the feeder. This will result in different voltage amplitudes and angles at different locations along the feeder. This phenomenon can result in high voltage imbalance especially at the end of the feeders. To keep the voltage drop within the limit all along the feeder, the utilities install single-phase pad mounted capacitors or increase the cross-section of the feeder. However, voltage imbalance at the end of the feeder still remains higher than the beginning of the feeder. This might cause a problem if some three-phase induction motors or power electronics based equipment are located far from the beginning of the feeder.

For example, in the network under consideration, the voltage amplitude at the beginning of the feeder is 0.975, 0.970 and 0.96 pu for phases *A*, *B* and *C* respectively. These values are decreased to 0.95, 0.92 and 0.90 pu at the end of the feeder, respectively. There-

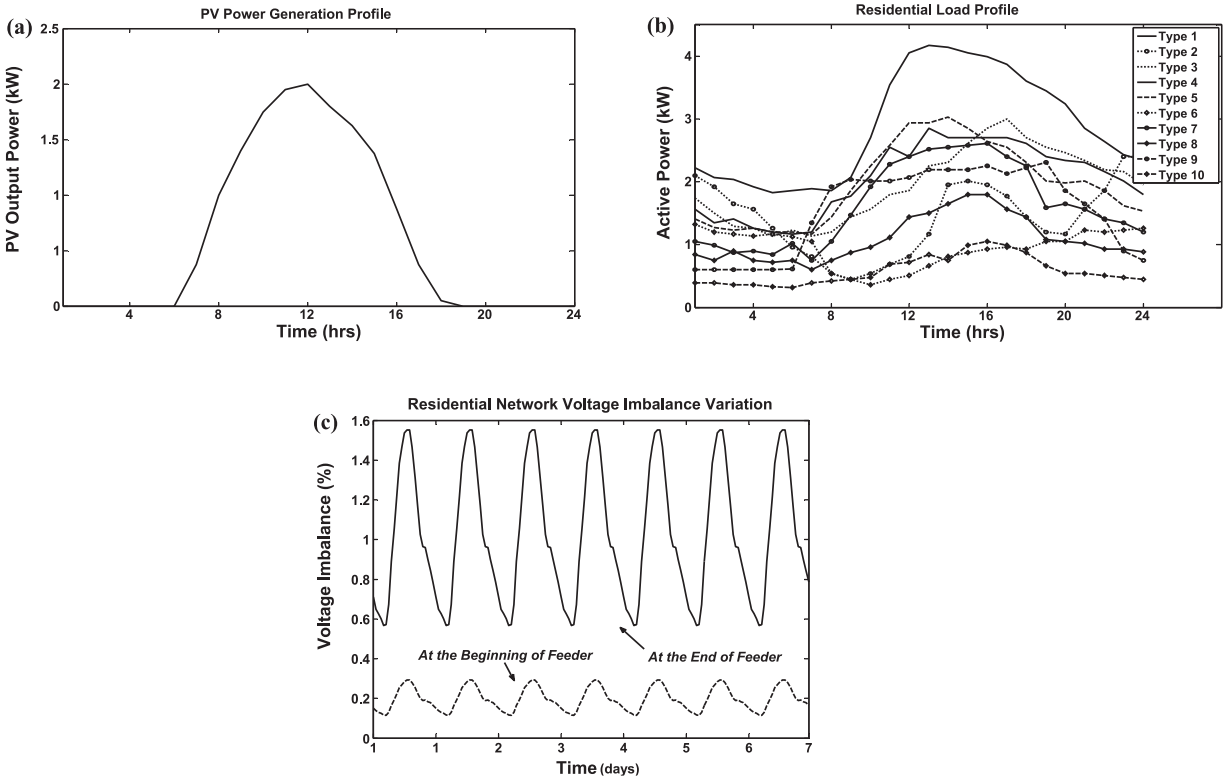

Fig. 4. (a) Power generation profile of a 2 kW rooftop PV, (b) 10 different types of residential loads profiles, (c) Time varying characteristic of voltage imbalance with constant location for PVs in the network.

fore, voltage imbalance at the beginning of the feeder has increased from 0.45% to 1.62% at the end.

Due to time varying characteristic of residential load demand and PV output power, a study is included to investigate the voltage imbalance variation during a specific time period. Let us assume some PVs with the power output profile as shown in Fig. 4a and the residential loads with load profile as shown in Fig. 4b are considered [23,24]. The time varying characteristic of VUF at the beginning and end of the feeder is shown in Fig. 4c. VUF will have a time varying characteristic but its value might increase depending on the location and ratings of the PVs.

4.1. Case 1 – sensitivity analysis of a single PV on voltage imbalance

The voltage imbalance variation due to the location of one PV with a constant rating will depend on the total load of the phase in which it is installed. Usually rooftop PVs can have ratings up to 5 kW for urban residential customers. It is also important to define the point at which the voltage imbalance will be measured.

It is expected that the voltage profile will improve in the phase the PV is installed. Let us consider either a 1 kW or a 5 kW PV installation at the beginning, middle and end of a feeder. In Fig. 5, the voltage profile of phase *A* is shown. As expected, the voltage amplitude increases with PV of higher ratings or when it is installed at the end.

The installation of a PV in a low load phase (phase *A* in this case) results in the increase in voltage difference and hence voltage imbalance at the end of the feeder while having minor effect at the beginning of the feeder. This voltage imbalance is more if the PV is installed at the end of the feeder or if the rating of the PV is high. The sensitivity analysis of voltage imbalance (calculated at the end of the feeder) versus the location and rating of rooftop PV installed in low load phase *A* is shown in Fig. 6a.

The voltage difference between the phases reduces if the PV is installed in high load phase (phase *C*). The decrease is more pronounced at the end of the feeder than at the beginning. This decrease at the end of the feeder is more if the PV is installed at the end of the feeder or if the rating of the PV is high. The sensitivity analysis of voltage imbalance (calculated at the end of the feeder) versus the location and rating of rooftop PV installed in low load phase *C* is illustrated in Fig. 6b.

These results prove that a rooftop PV (with a rating of less than 5 kW) can cause network voltage imbalance to increase by 0.1% when installed at the beginning of the feeder and by 25% when installed at the end of the feeder, specifically when the feeder supplies up to 1 MW load. For example, in the worst case, the VUF figure of 1.62% without any PV increased to 2.02% (i.e., a 25% rise) when a 5 kW PV was installed at the end of the feeder. Even in this worst case, the VUF, at the end of the feeder, is not significant since

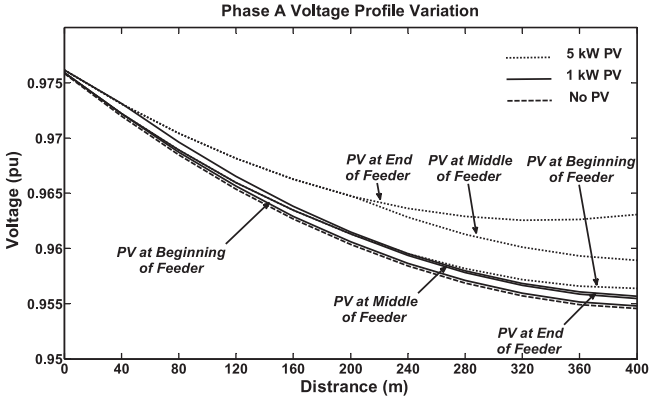

Fig. 5. Variation of phase *A* voltage profile versus the location and rating of the PV in phase *A*.

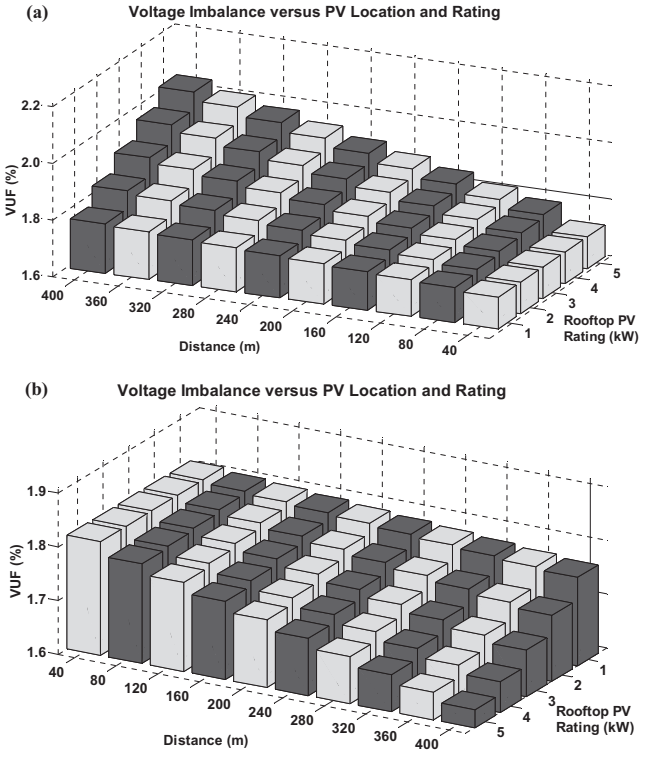

Fig. 6. Voltage imbalance sensitivity analysis versus PV location and rating in (a) low load phase – Phase *A*, (b) high load phase – Phase *C*.

it still does not lead to non-standard voltage imbalance. However, this may not be true when more than one PV get installed in the network.

4.2. Case 2 – mutual effect of PVs on voltage imbalance

In this part, it is assumed that a number of PVs are installed only in one phase of the network. Note that there are three feeders and the PVs will be installed in only the low load phase (*A*) in each of these feeders.

Fig. 7a shows the voltage imbalance in feeder 1 both at the beginning and end of the feeder. We first add PVs to phase *A* of feeder-1, one at a time with the maximum number being 10. Then the PVs in the other two feeders are added in the same manner. During this, the size of the PVs, varying from 1 kW to 5 kW, is assumed to be the same. It can be seen that VUF in feeder-1 rises rapidly as the PVs are added. However, adding PVs in the other two feeders does not cause a significant increase in the VUF in feeder-1. Also it can be seen that VUF increases with the size of the PVs. Moreover, note that VUF at the beginning of the feeder does not change much.

Fig. 7b shows VUF at the end of all three feeders when the 5 kW PVs are installed in phase *A*. This figure overlays the plot similar to those shown in Fig. 7a for all the three feeders. It is evident that VUF in each of the feeders increase significantly when PVs are installed in the feeder itself and rises at a slow rate when the PVs are installed in the other feeders.

Fig. 8 shows the effects of adding PVs in the high load phase (phase *C*). It can be seen from this figure that for smaller PVs (1 and 2 kW), the VUF decreases continuously. However for PVs of rating 3 kW and higher, VUF decreases up to a point, beyond which it rises sharply. The reason for this is that as the PV ratings increase, the power generated becomes higher than the load demand of the phase. This causes the phase voltage angle to differ from 120° resulting in higher VUF.

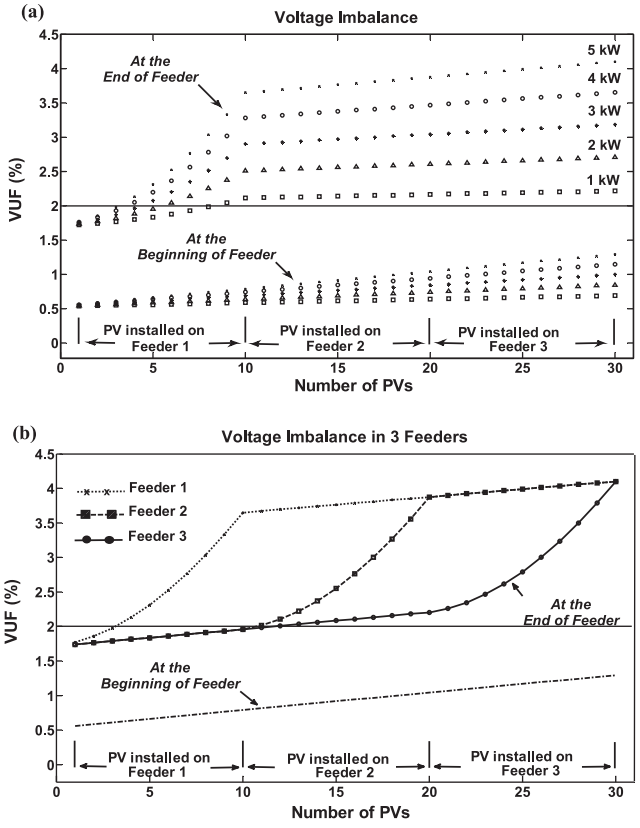

Fig. 7. Network voltage imbalance variations based on the location and rating effects of the PVs in phase *A* of all three feeders: (a) calculated in feeder 1, (b) calculated on all feeders.

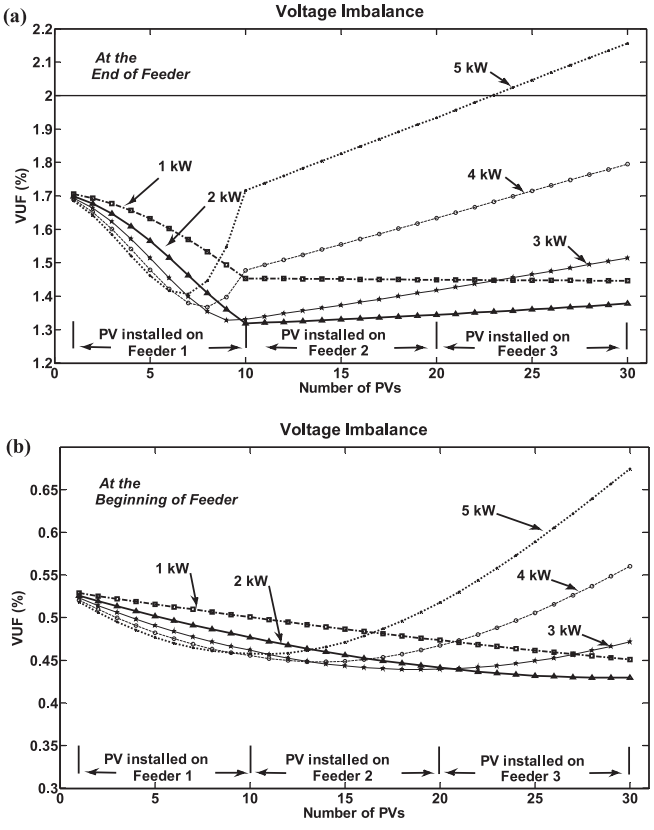

Fig. 8. Network voltage imbalance variations based on the location and rating effects of the PVs in phase *C* of all three feeders: (a) in the beginning of feeder 1, (b) at the end of feeder 1.

Table 1
Numerical voltage imbalance.

PV installed in		Low load phase		High load phase	
Total PV power		Feeder beginning	Feeder end	Feeder beginning	Feeder end
10 kW	2 × 5	0.42	1.87	0.36	1.34
	2 × 5	0.43	2.00	0.35	1.29
	2 × 5	0.43	2.00	0.35	1.29
	5 × 2	0.43	2.00	0.35	1.26
	5 × 2	0.43	1.95	0.35	1.27
	5 × 2	0.45	2.13	0.34	1.19
	10 × 1	0.41	1.83	0.36	1.32
20 kW	4 × 5	0.47	2.22	0.34	1.22
	4 × 5	0.51	2.81	0.33	1.27
	4 × 5	0.54	3.02	0.32	1.37
	5 × 4	0.52	2.92	0.32	1.31
	5 × 4	0.51	2.73	0.33	1.23
	5 × 4	0.51	2.73	0.33	1.23
	10 × 2	0.45	2.14	0.34	1.19
	20 × 1	0.53	2.20	0.31	1.22

Another study is performed to find out the effects of number of PVs installed on a phase of a feeder while their total power injection to the grid remains constant, either at 10 kW or 20 kW. The results are shown in Table 1 which highlight the importance of the location of PV installation. For example, if 2 × 5 kW PVs are installed on nodes 1, 10 or 2, 10 or 5, 10, they will result in different values of voltage imbalance. Now if the PVs are chosen 5 × 2 kW, the voltage imbalance might have increased or decreased compared to the previous situation. Therefore, making a general conclusion about voltage imbalance for different numbers of PVs on one phase but with constant total injected power seems to be impossible without taking into account their locations. Hence, through Fig. 6 and Table 1, it can be concluded that the voltage imbalance is greater if PVs with constant total power injection are installed at the end of the feeder comparing to when installed at the beginning.

4.3. Case 3 – stochastic evaluation of voltage imbalance

A stochastic evaluation is carried out for investigating the uncertainties in the network. In this study, it is assumed the PVs (with rating of 1, 2, 3, 4, 5 kW) have equal probability of 20% each, as shown in Fig. 3. The uncertainty in the PV rating is modelled by drawing a random number U_1 distributed uniformly under [0,1]. Using U_1, the instantaneous output power of each PV is selected in 0–5 kW range during day-night period. The uncertainty of PV location along the feeder [0–400 m], is modelled by drawing a random number U_2 distributed uniformly under [0,1]. This is done for all phases and feeders of the studied network independently.

The number of the householders with installed rooftop PVs is assumed to be 1/4, 1/2 and 3/4 of the total number of householders as 3 different scenarios, shown in Fig. 3. For selecting 1 out of these 3 scenarios, a random number U_3 distributed uniformly under [0,1] is used. If $U_3 < 0.33$ then scenario 1 is selected, if $0.33 \leq U_3 \leq 0.66$ then scenario 2 is selected and if $U_3 > 0.66$ then scenario 3 is selected.

Another study was also carried out with normal distributions for U_1 with ($\mu = 0.5$ and $\sigma = 0.2$) and also U_3 with ($\mu = 0.3$ and $\sigma = 0.08$) that due to similarity in the results are not shown here.

This study was carried out for several times with minimum number of $N = 10{,}000$ trials. A sample result for the scenario of 1/2 householders having PV are shown in Fig. 9a. It can be seen that the voltage imbalance calculated at the beginning of the feeder always remain about 0.8%. This value for the end of the feeder varies between 1 and 3%.

The PDFs for the cases when 1/2 of the householders have PVs is shown in Fig. 9b. The PDFs for all the three cases have mean value (λ) equal to 0.61% at the beginning of the feeder and 1.80% at the end of the feeder.

From Fig. 9b, it can be seen that, there is a high probability that the voltage imbalance at the end of the feeder is more than the 2% standard limit. This probability is referred to as the failure index (F_I%) which is the frequency of the cases in the shaded area in probability density function and is calculated as

$$F_I\% = \text{shaded area} \times 100 \tag{10}$$

While voltage imbalance failure index is zero at the beginning of the feeder, it is about 30.19% at the end of the feeder.

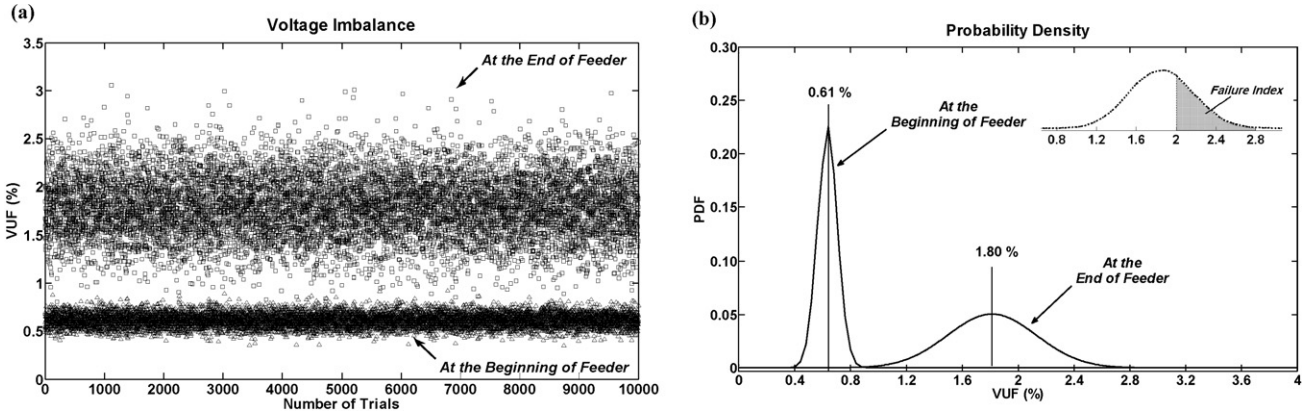

Fig. 9. (a) Voltage imbalance for 10,000 scenarios of random location and ratings of PVs. (b) Probability density function of voltage imbalance.

Table 2
λ and failure indices of voltage imbalance of the studied LV distribution network for different residential load levels.

Residential load status	Highly unbalanced	Lightly unbalanced	Almost balanced
λ at beginning of feeder	0.66	0.58	0.46
λ at end of feeder	1.92	1.70	1.37
Failure Index (F_I%)	46.0	22.3	6.0

Table 3
λ and failure indices of voltage imbalance of the studied network considering majority of PVs installed at beginning or end of the feeder.

Majority of PVs installed at	Beginning of feeder	Middle of feeder	End of feeder
λ at beginning of feeder	0.61	0.61	0.62
λ at end of feeder	1.88	1.97	2.06
Failure Index (F_I%)	16.2	51.8	67.9

The customer load consumption is different at different times. Therefore, the residential loads also have an effect on the VUF. This phenomenon is included as the fourth uncertainty condition for Monte Carlo method. The results of this analysis are given in Table 2 for different load consumption levels in the network during different times. It can be seen that when the loads are almost balanced, λ and failure index decrease while they increase if the loads are highly unbalanced.

The influence of the location of the PVs (at the beginning or end of the feeder) on voltage imbalance is discussed before. In the previous studies, it was assumed the PVs are distributed randomly along the feeder. It is of high interest to investigate the case when the majority of the PVs are installed at the beginning or at the end of the feeder. Therefore, another Monte Carlo study is carried out to investigate this phenomenon. The results of this study given are in Table 3. It can be seen that generally when the majority of the PVs are installed at the end of the feeder, the failure index and λ increase at the end points of the network.

5. Improvement methods

Based on the probabilistic and numerical results of Section 4, it can be concluded that the voltage imbalance at the beginning of the feeder, regardless of the location, number and rating of the installed rooftop PVs, is likely to be less than 1%. However, the voltage imbalance at the end of the feeder can be more than 2% for 30.19% of the cases. To reduce this imbalance, four improvement methods are discussed below, including one proposed PV converter control method.

5.1. Methods

The four improvement methods are discussed below.

(1) *Increasing feeder cross-section*: This will result in reducing the voltage drop along the feeder and therefore, there will be little difference among the voltage amplitude of three phases of a feeder at the end.
(2) *Installing capacitors*: Installation of pad mounted switched capacitors in the LV feeders. It is important to note that if a three-phase capacitor is installed on a LV feeder, the voltage imbalance will almost remain the same. However, if a capacitor is connected only on a phase at a point where the voltage is below 0.95 pu, the voltage profile of the phase can be improved.
(3) *Both feeder cross-section increase and capacitor installation*: This is a combination of the above two methods.
(4) *A new control scheme for PV converters*: The previous three methods mentioned above will increase the cost of installations. Instead a new converter control strategy is presented below which will incur no additional cost. If the PV converter is controlled appropriately to regulate the voltage of the feeder, it can result in voltage profile improvement which can reduce VUF. In general, PV converters are controlled such that they inject constant active power with zero reactive power (termed as constant PQ mode here). Instead, the voltage can be regulated if reactive power can also be supplied by these converters.

The proposed scheme controls the injected amount of reactive power of the PV based on the amplitude of the voltage of the feeder at the point of common coupling.

For this purpose, it is necessary to control the voltage amplitude ($|V_{PV,k}|$) and angle ($\delta_{PV,k}$) at the output of the converter (as shown in Fig. 2). The controller should generate $|V_{PV,k}|$ and $\delta_{PV,k}$ accurately so that the injected $Q_{PV,k}$ will lead to increase of feeder voltage amplitude $|V_k|$ to a desired value (let us say 0.95–0.96 pu) while its active power output $P_{PV,k}$ remains equal to maximum PV active power output. Let us assume

$$\left|V_{PV,k}\right| = \left|V_{ref}\right| + n.Q_{PV,k} \tag{11}$$

where $|V_{ref}|$ is equal to $|V_{PV,k}|$ when the PV operates in UPF mode with $Q_{PV,k} = 0$ and n is a coefficient. Substituting (11) in PV power flow equations (4) and (5), we get

$$P_{PV,k}.X_{PV,k} = |V_k|(|V_{ref}| + n.Q_{PV,k})\sin(\delta_{PV,k} - \delta_k) \tag{12}$$

$$Q_{PV,k} = \frac{\left|V_k\right|(|V_{ref}| + n.Q_{PV,k})\cos(\delta_{PV,k} - \delta_k) - |V_k|^2}{X_{PV,k}} \tag{13}$$

Denoting angle difference $\delta_d = \delta_{PV,k} - \delta_k$ (see Fig. 2), from (11), $Q_{PV,k}$ can be solved as

$$Q_{PV,k} = \frac{|V_k||V_{ref}|\cos\ \delta_d - |V_k|^2}{X_{PV,k} - n|V_k|\cos\ \delta_d} \tag{14}$$

Substituting (14) in (12), we get

$$\begin{aligned} P_{PV,k}X_{PV,k} &= |V_k|(|V_{ref}| + nQ_{PV,k})\sin\ \delta_d \\ &= |V_k| \times \left(|V_{ref}| + \frac{n|V_k||V_{ref}|\cos\ \delta_d - n|V_k|^2}{X_{PV,k} - n|V_k|\cos\ \delta_d}\right)\sin\delta_d \\ &= |V_k| \times \left(\frac{|V_{ref}|X_{PV,k} - n|V_k|^2}{X_{PV,k} - n|V_k|\cos\ \delta_d}\right)\sin\ \delta_d \end{aligned} \tag{15}$$

For small values of δ_d, we have $\cos(\delta_d) = 1$ and $\sin(\delta_d) = \delta_d$. Therefore, from (15) we get

$$\delta_d = \frac{P_{PV,k}X_{PV,k}(X_{PV,k} - n|V_k|)}{|V_k|(|V_{ref}|X_{PV,k} - n|V_k|^2)} \tag{16}$$

where the approximation has error less than 1% for $\delta_d \le 15^\circ$.

Table 4
λ and failure indices of voltage imbalance of the studied LV distribution network for three improvement methods.

	Nominal case	Method-1 (cross-section increase)	Method-2 (capacitor placement)	Method-3 (cross-section and capacitor)	Method-4 (converter control)
λ at beginning of feeder	0.61	0.61	0.47	0.47	0.16
λ at end of feeder	1.80	1.58	1.37	1.20	0.23
Failure Index (F_I%)	30.19	8.6	3.5	0	0

5.2. Numerical results

To verify the efficacy of these methods, another set of stochastic studies are carried out. The results for the first three methods are given in Table 4. In this, the nominal case indicates when the feeder cross-section is 70 mm^2 and no capacitors are installed in the system. These are obtained from Fig. 9(b). For method (1) mentioned above, the feeder cross-section is increased to 95 mm^2. The failure index reduces to 8.6%. For method (2), a 15 kVAr capacitor is installed at the 2/3rd distance from the beginning of the feeder. The failure index reduces to 3.5%. For method (3), both feeder cross-section has been increased to 95 mm^2 and a 15 kVAr capacitor is installed at the 2/3rd distance from the beginning of the feeder. In this case, the failure index is zero.

As mentioned earlier, the previous three methods will increase the cost of installation. This can be avoided by using the proposed converter control scheme. For method (4), let us assume the presence of three 1 kW rooftop PVs with proposed control scheme at the end points of one of the feeders. Since the voltage amplitude of the three phases where about 0.95, 0.92 and 0.90 pu at the end nodes, all the PVs have worked in the proposed control scheme to increase it to 0.96 pu on all phases. In this way, the voltage amplitude at the end node of for all three phases increase to 0.96 pu and VUF decreases to 0.23%.

A stochastic study has also been conducted to verify its performance for different scenarios of PVs installed in different locations and ratings in the network while three 1 kW rooftop PVs are installed always at the end of the three phases. The results of this study are shown in Fig. 10. It can be seen that λ reduces significantly from 0.61 to 0.16% at the beginning of the feeder and from 1.80 to 0.23% at the end of the feeder. The failure index for this case is zero.

The failure index and λ values for the network with four different improvement methods are given in Table 4. The efficacy of the discussed improvement methods is obvious from this table. Comparing the results in Table 4, it can be concluded that the proposed converter method has the highest effect on voltage imbalance reduction along the whole feeder with minimum costs applied to the network.

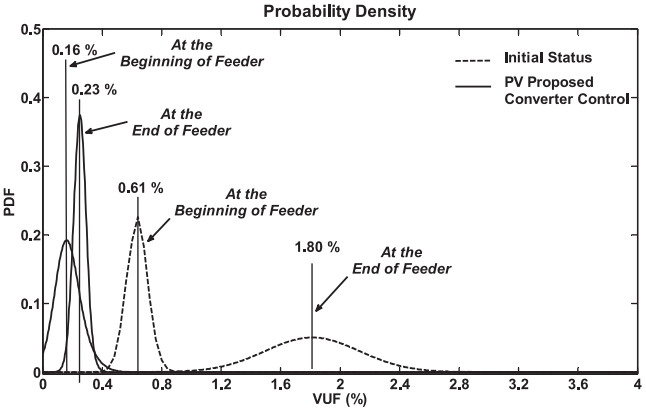

Fig. 10. Probability density function of voltage imbalance with the proposed control scheme.

Table 5
Failure indices of voltage imbalance of the studied LV distribution network for different capacity levels of the converter.

Injected Q/rated P	Converter capacity increase (%)	Failure index (F_I%)
0	0	30.19
0.2	1.98	23.0
0.4	7.70	12.8
0.6	16.62	1.8
0.8	28.06	0
1	41.42	0

The main drawback of the proposed converter control method is the need to increase the capacity of the converter. Since PVs are owned and operated by the customer, this will increase the investment cost. Therefore, it is important to investigate an optimum capacity for the converters (i.e. the amount of reactive power that can be supplied by the converter to the grid). A study has been carried out to investigate the effect of limiting the capacity of the converter on the VUF. This result is shown in Table 5. It can be seen that with a 16.62% increase in the capacity of these converters, failure index can be decreased from 30.19% to 1.8%.

The Simulations have taken into account the real network conditions and technical parameters including network, PV, converter and load pattern. Therefore, the analytical extrapolation is expected to have low uncertainty.

6. Conclusions

A voltage imbalance sensitivity analysis and stochastic evaluation based on the rating and location of single-phase grid-connected rooftop PVs in a residential LV distribution network are presented. Through the studies, it is proved that rooftop PV installation will have minor effect on the voltage imbalance at the beginning of a LV feeder designed with engineering judgments. However, it might increase at the end of the feeder to more than the standard limit. It is also proved that depending on the load of the phase in which the PV is installed, the voltage imbalance will increase or decrease based on the location and rating of the PVs. If a PV is installed on one feeder, the voltage imbalance will be modified on all the other LV feeders of the network. Based on the numerical results, a generalized characteristic of voltage imbalance of LV residential networks due to rooftop PV installation is presented. The stochastic simulation demonstrated that the failure index of non-standard voltage imbalance in these networks is high (30.19%). Improvement methods are investigated and a new control scheme for PV converter is proposed and its efficacy is verified by the stochastic and numerical results.

Acknowledgment

This project was supported financially by Australian Research Council through the ARC Discovery Grant DP 0774092.

Table 6
Convergence of Monte Carlo method for different trial numbers.

N (trial number)	Failure index (FI) [%]	λ at beginning of feeder	λ at end of feeder	Var(VUF) at beginning of the feeder [%]	Var(VUF) at the end of feeder [%]	Error [%] of end Var(VUF) to other trial numbers
1000	4.9000	0.3846	1.5425	0.1692	5.9295	26.28
5000	4.3400	0.3849	1.5309	0.1714	6.0554	24.71
10,000	6.8900	0.3864	1.5363	0.1905	8.0436	0
20,000	6.9900	0.3865	1.5346	0.1883	7.9531	1.12
30,000	7.0367	0.3867	1.5342	0.1900	8.0176	0.32
50,000	7.0700	0.3859	1.5328	0.1886	8.1231	0.98
75,000	6.9693	0.3864	1.5333	0.1896	8.0754	0.39
100,000	7.0040	0.3862	1.5336	0.1896	8.0561	0.15

Table 7
Technical parameters of the studied LV distribution network.

Transformer	11/0.415 kV, 500 kVA, $\Delta/Y_{grounded}$, $x = 0.04$ pu
MV feeder	Three-phase 11 kV radial Supplying 4 transformers with total demand of 1 MVA 50 mm^2 ACSR, 2 km overhead line $(z = 1.08 + j \times 0.302)\,\Omega$/km
LV feeder	3 feeders, each 3-phase 4-wire, 415 V Each with a length of 400 m long Aerial bundle cable 70 mm^2 $(z = 0.551 + j \times 0.088)\,\Omega$/km for phase wires and 35 mm^2 $(z = 0.65 + j \times 0.09)\,\Omega$/km for neutral wire
Residential load type 1	20 one kW residential loads on each feeder (all on phase A) $\cos\varphi = 0.95$, $z = 51.9840 + j \times 17.0863\,\Omega$ Two loads connected to each pole, next pole distance 40 m
Residential load type 2	20 two kW residential loads on each feeder (all on phase B) $\cos\varphi = 0.95$, $z = 25.9920 + j \times 8.5432\,\Omega$ Two loads connected to each pole, next pole distance 40 m
Residential load type 3	20 three kW residential load on each feeder (all on phase C) $\cos\varphi = 0.95$, $z = 17.3280 + j \times 5.6954\,\Omega$ Two loads connected to each pole, next pole distance 40 m
Rooftop PV	1–5 kW, unity power factor, $L = 5$ mH

Appendix A.

(i) Monte Carlo Method Convergence

The stopping rule of the Monte Carlo method is chosen based on achieving an acceptable convergence for $\overline{VUF}$ and Var(VUF). In this study, the program was rerun for several trial numbers. The mean (λ) and Var(VUF) at the beginning and end of feeder in addition to Failure Index (F_I%)for different trial numbers is listed in Table 6. From this table, it can be seen that the mean, variance and failure index values do not vary much after N = 10,000 trials. The error value in Var(VUF) is given in the last column of the table assuming the base case of 10,000 trials. It can be seen that an increase in trial number from 10,000 does not increase the error in variance significantly. Therefore this value is chosen as the stopping rule.

(ii) Technical parameters of the studied network (Table 7).

References

[1] A. Ghosh, G. Ledwich, Power quality enhancement using custom power devices, Kluwer Academic Publishers, 2002, ISBN: 1402071809.

[2] T.A. Short, Electric Power Distribution Handbook, CRC Press, 2004.

[3] A.V. Jouanne, B. Banerjee, Assessment of voltage imbalance, IEEE Trans. Power Deliv. 16 (October (4)) (2001) 782–790.

[4] P. Gnacinski, Windings temperature and loss of life of an induction machine under voltage unbalance combined with over- or undervoltages, IEEE Trans. Energy Convers. 23 (2) (2008) 363–371.

[5] PVPS Annual Report – Implementing Agreement on Photovoltaic Power Systems, International Energy Agency (IEA) – Photovoltaic Power Systems Programme, 2008.

[6] M. A. Eltawil and Z. Zhao, Grid-connected photovoltaic power systems: Technical and potential problems-A review, Renew. Sust. Energy Rev., vol. 14, pp. 112-129, 2010.

[7] S.A. Papathanassiou, A technical evaluation framework for the connection of DG to the distribution network, Electr. Power Syst. Res. 77 (2007) 24–34.

[8] J.A.P. Lopes, N. Hatziargyriou, J. Mutale, P. Djapic, N. Jenkins, Integrating distributed generation into electric power systems: a review of drivers, challenges and opportunities, Electr. Power Syst. Res. 77 (2007) 1189–1203.

[9] P. Trichakis, P.C. Taylor, L.M. Cipcigan, P.F. Lyons, R. Hair, T. Ma, An investigation of voltage unbalance in low voltage distribution networks with high levels of SSEG, Proceedings of the IEEE 41st International Universities Power Engineering Conference (UPEC) 41 (September) (2006) 182–186.

[10] P. Trichakis, P.C. Taylor, P.F. Lyons, R. Hair, Predicting the technical impacts of high levels of small-scale embedded generators on low voltage networks, IET Renew. Power Gen. 2 (4) (2008) 249–262.

[11] W. Li, Risk Assessment of Power Systems: Models, Methods, and Applications, Wiley Publishers, 2005, ISBN: 047163168X.

[12] A.K. Singh, G.K. Singh, R. Mitra, Some observations on definitions of voltage unbalance, in: 39th North American Power Symposium (NAPS), September/October 2007, pp. 473–479.

[13] D.C. Garcia, A.L.F. Filho, M.A.G. Oliveira, O.A. Fernandes, F.A. do Nascimentoa, Voltage unbalance numerical evaluation and minimization, Electr. Power Syst. Res. 79 (2009) 1441–1445.

[14] P.G. Kini, R.C. Bansal, R.S. Aithal, A novel approach toward interpretation and application of voltage unbalance factor, IEEE Trans. Ind. Electron. 54 (4) (August 2007) 2315–2322.

[15] IEEE Recommended Practice for Monitoring Electric Power Quality, IEEE Standard 1159–1995.

[16] Planning Limits for Voltage Unbalance in the United Kingdom, The Electricity Council, Engineering recommendation P29, 1990.

[17] Electric Power Systems and Equipment-Voltage ratings (60 Hz), ANS Standard C84.1-1995.

[18] IEEE Recommended Practice for Electric Power Systems in Commercial Building (Gray Book), IEEE Std 241-1990.

[19] K. Lee, G. Venkataramanan, T. Jahns, Source current harmonic analysis of adjustable speed drives under input voltage unbalance and sag conditions, IEEE Trans. Power Deliv. 21 (2) (2006) 567–576.

[20] P.V.S. Valois, C.M.V. Tahan, N. Kagan, H. Arango, Voltage unbalance in low voltage distribution networks, in: Proceedings of the 16th International Conferene on Electricity Distribution (CIRED), 2001.

[21] Power Quality Measurement Results in 120 Points in Eastern Azarbayjan Electric Power Distribution Co., Technical report, 2008 (in Persian).

[22] IEEE Recommended Practice for Utility Interface of Photovoltaic (PV) Systems, IEEE Standard 929-2000.

[23] G. Makrides, B. Zinsser, M. Norton, G.E. Georghiou, M. Schubert, J.H. Werner, Potential of photovoltaic systems in countries with high solar irradiation, Renew. Sust. Energy Rev. (14) (2010) 754–762.

[24] D. Parker, M. Mazzara, J. Sherwin, Monitored energy use patterns in low-income housing in a hot and humid climate, in: Proceedings of the 10th Symposium on Improving Building Systems in Hot Humid Climates, 1996.